Two-Dimensional Tensor Product Variational Formulation

Tomotoshi Nishino,[*] Yasuhiro Hieida, Kouichi Okunishi[1,2], Nobuya Maeshima[3], Yasuhiro Akutsu[3], and Andrej Gendiar[4]

Department of Physics, Graduate School of Science, Kobe University, 657-8501
[1] *Department of Applied Physics, Graduate School of Engineering, Osaka University, 565-0781*
[2] *Department of Physics, Faculty of Science, Niigata University, 950-2181*
[3] *Department of Physics, Graduate School of Science, Osaka University, 560-0043*
[4] *Institute of Physics, Slovak Academy of Sciences, Dúbravská cesta 9, SK-842 28 Bratislava, SLOVAKIA*

(Received)

We propose a numerical self-consistent method for 3D classical lattice models, which optimizes the variational state written as two-dimensional product of tensors. The variational partition function is calculated by the corner transfer matrix renormalization group (CTMRG), which is a variant of the density matrix renormalization group (DMRG). Numerical efficiency of the method is observed via its application to the 3D Ising model.

§1. Introduction

Variational states represented as products of local tensols have been used widely for calculating the ground-state energy in one-dimensional (1D) quantum systems and the free energy in two-dimensional (2D) classical statistical systems. In 1941 Kramers and Wannier calculated a lower bound of the partition function of the 2D Ising model using the matrix product state,[1] which is a prototype of the tensor product state (TPS). A remarkable point in their variational approach is that the calculated lower bound is a good approximation for the exact partition function[2] especially in low and high temperature regions. About 30 years later Baxter formulated a variational method, which is a natural extension of the Kramers-Wannier approximation, by expressing the eigenstate of the transfer matrix in the form of TPS.[3]-[5] He has also shown that the integrable model can be solved using the corner transfer matrix generated from a local tensor with infinite degree of freedom. Quite recently the density matrix renormalization group (DMRG)[6]-[8] has provided a very practical numerical procedure to perform the variational computation for the position-dependent TPS.[9]-[11]

A current interest about TPS is its application to higher dimensional systems.[8],[12],[13] For example, Niggemann *et al* has shown that the ground state of the 2D valence-bond-solid (VBS) type quantum spin model is exactly expressed as the TPS, where the calculation of the ground-state expectation value is reduced to that of the partition function for the corresponding 2D vertex model.[14],[15] Hieida *et al* evaluated the

---

[*] E-mail address: nishino@phys.sci.kobe-u.ac.jp

correlation function of the 2D deformed VBS model by combining DMRG with the *exact* variational formulation of the system.[16] Also for the 3D classical models, the authors have been generalizing the 2D TPS, in the context of the higher-dimensional DMRG.[13,17,18]

In constructing the TPS, the most important step is how to represent the local tensors, since it often reflects on the efficiency of the variational calculation. In our previous works, we calculated the variational free energy of the 3D Ising model, employing the interaction-round-a-face (IRF) representation of the local tensor with 16 variational parameters.[18] Such a variational state is often called as the IRF-type TPS.[12,18] The resulting efficiency is quite good in the off-critical region, though the calculated transition temperature is about 1.5% higher than that obtained by the Monte Carlo (MC) simulations.[19,20] However, we have only discussed the efficiency of the IRF-type TPS and thus it is necessary to challenge another type of TPS.

In this paper, we construct the vertex-type TPS in 2 dimension, by introducing four auxiliary variables of m-states into a local tensor. The new variational state has $2m^4$ parameters, which is twice as many as that of the IRF-type TPS when $m = 2$. Numerical efficiency of this TPS is examined through its application to a 3D vertex model whose thermodynamic property is equivalent to the 3D Ising model.[21] In the next section, we show the construction of the 2D TPS with auxiliary variables. Numerical procedures to obtain the maximum of the variational partition function is shown in §3, and the calculated result is explained in §4. Conclusions are summarized in §5.

§2. Variational Formulation

As an example of the 3D classical model, we consider the 3D vertex model that has one-to-one correspondence with the simple cubic lattice Ising model.[21] Let us start from a brief description of this vertex model. Consider a simple cubic lattice of the size $N \times N \times \infty$ in the XYZ-directions, where a 2-state spin variable that takes either up (+) or down (−) are sitting on each link between the nearest lattice points. Thus one lattice point is surrounded by 6 spins as shown in Fig. 1. This is the unit of the 3D vertex model, which is called a 'vertex'. We label the spins on the vertical links of the vertex as s (bottom) and $\bar{s}$ (top), and those on the horizontal links as σ, σ', σ'', and σ'''.

Statistical property of the vertex model is specified by the Boltzmann weight $w_{\bar{s}s}(\sigma\,\sigma'\sigma''\sigma''')$ assigned to the vertex. In the following, we set the weight as

$$w_{\bar{s}s}(\sigma\,\sigma'\sigma''\sigma''') = \sum_{x=\pm 1} U_{\bar{s}}^x\, U_s^x\, U_\sigma^x\, U_{\sigma'}^x\, U_{\sigma''}^x\, U_{\sigma'''}^x\,, \qquad (2\cdot1)$$

where U_y^x is unity when $x = y$ and is $e^{\beta J} + \sqrt{e^{2\beta J} - 1}$ otherwise; the 3D vertex model has the same free energy as the 3D Ising model with the Hamiltonian $\mathcal{H} = \sum J x x'$, where x and x' denote the neighboring Ising spin variables.[21]

Let us introduce two notations in order to simplify the following expressions. The first one is $\{\sigma\}$, which represents the group of horizontal spins $\sigma, \sigma', \sigma''$, and σ'''
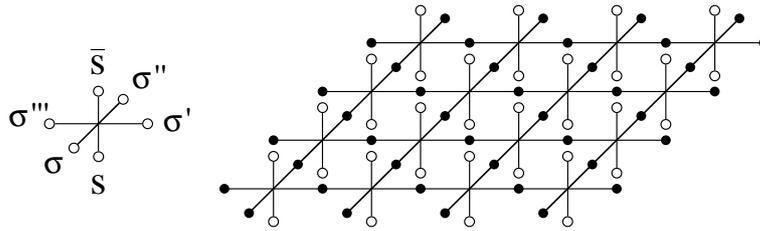
Fig. 1. Spin variables around a vertex, and the transfer matrix of the 3D vertex model.

around a vertex. For example, the vertex weight $w_{\bar{s}s}(\sigma\,\sigma'\sigma''\sigma''')$ is simply written as $w_{\bar{s}s}\{\sigma\}$. The second one is the matrix representation of the Boltzmann weight

$$W\{\sigma\} \equiv \left(\begin{array}{cc} w_{++}\{\sigma\} & w_{+-}\{\sigma\} \\ w_{-+}\{\sigma\} & w_{--}\{\sigma\} \end{array} \right),\qquad (2\cdot2)$$

where we have regarded s and $\bar{s}$ of $w_{\bar{s}s}\{\sigma\}$, respectively, as column and row indices of the 2×2 matrix.

The system explained above can be interpreted as the infinite stack of $N \times N$ layers, where each layer plays the role of the layer-to-layer transfer matrix T. Using the matrix expression in Eq. (2.2) and writing the vertex weight at the position (i, j) in the layer as $W\{\sigma_{ij}\}$, we can express the transfer matrix as a two-dimensionally connected vertices:

$$T \equiv \sum_{[\sigma]} \prod_{1 \leq ij \leq N} W\{\sigma_{ij}\},\qquad (2\cdot3)$$

where $\sum_{[\sigma]}$ denotes the configuration sum for all the spins on the horizontal links, that are shown by black circles in Fig. 1. (We use black marks for the spin variables whose configuration sums are taken.) Our interest is to calculate the variational partition function per layer

$$\lambda[\Psi] = \frac{\langle\Psi|T|\Psi\rangle}{\langle\Psi|\Psi\rangle}\qquad (2\cdot4)$$

for a given TPS $|\Psi\rangle$, and further to find out the best TPS that minimizes $\lambda[\Psi]$.
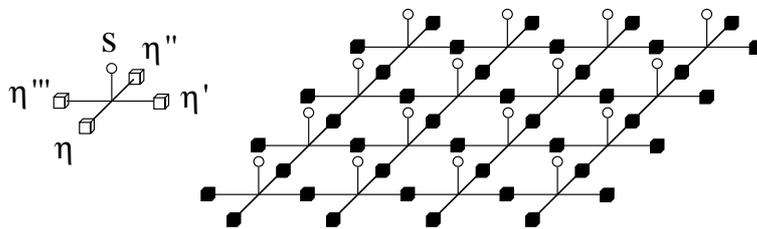

Fig. 2. Spin variables around a variational tensor, and the variational state constructed as 2D product of the tensors.

Now we explicitly construct the trial eigenvector $|\Psi\rangle$ as the 2D tensor product, as is shown in Figure 2.[12), 18)] Each tensor has an apex spin $s = \pm 1$ and four m-state auxiliary variables η, η', η'', and η''' shown by cubes. Let us express the elements of the tensor as $v^s\{\eta\}$, where $\{\eta\}$ denotes the set of auxiliary variables η, η', η'', and η'''. As we have expressed the vertex weight as a matrix in Eq. (2.2), it is useful to interpret $v^+\{\eta\}$ and $v^-\{\eta\}$ as components of the column vector

$$\mathbf{V}\{\eta\} \equiv \left(\begin{array}{c} v^+\{\eta\} \\ v^-\{\eta\} \end{array} \right). \tag{2.5}$$

Using this notation, we construct the 2D TPS as

$$|\Psi\rangle \equiv \sum_{[\eta]} \prod_{1 \leq ij \leq N} \mathbf{V}\{\eta_{ij}\}, \tag{2.6}$$

where $\{\eta_{ij}\}$ denotes the set of auxiliary variables around the lattice point (i, j), and the configuration sum $\sum_{[\eta]}$ is taken over for all the auxiliary variables shown by black cubes in Fig. 2. Since the above construction of the TPS is similar to that of the transfer matrix T of the 3D vertex model, we call the TPS (2.6) as the *vertex-type* TPS.[12), 18)]
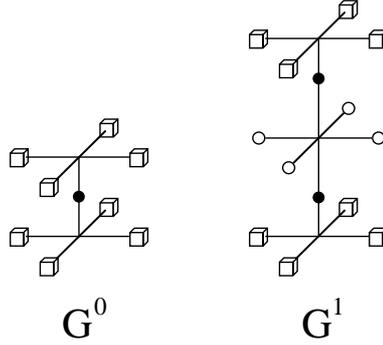

$$\mathbf{G}^0 \qquad\qquad \mathbf{G}^1$$

Fig. 3. The vertex weight G^0 of the 2-layer classical system (Eq. (2.9)), and G^1 of the 3-layer one (Eq. (2.10)).

The main profit of expressing the variational state in the form of the TPS is that both $\langle\Psi|\Psi\rangle$ and $\langle\Psi|T|\Psi\rangle$ can be expressed as the partition functions of 2- and 3-layer 2D classical lattice models, respectively.[14), 16) - 18)] Let us consider $\langle\Psi|\Psi\rangle$ first. From the definition of $|\Psi\rangle$ in Eq. (2.6) we obtain

$$\langle\Psi|\Psi\rangle = \sum_{[\eta]\,[\bar\eta]} \prod_{1 \leq ij \leq N} \mathbf{V}\{\bar\eta_{ij}\} \cdot \mathbf{V}\{\eta_{ij}\} = \sum_{[\eta]\,[\bar\eta]} \prod_{1 \leq ij \leq N} \left(\sum_{s=\pm 1} v^s\{\bar\eta_{ij}\} v^s\{\eta_{ij}\} \right), \tag{2.7}$$

where the configuration sum is taken over for all the spins and the auxiliary variables. Introducing the new notation

$$G^0\{\bar\eta_{ij}|\eta_{ij}\} \equiv \mathbf{V}\{\bar\eta_{ij}\} \cdot \mathbf{V}\{\eta_{ij}\} = \sum_{s=\pm 1} v^s\{\bar\eta_{ij}\} v^s\{\eta_{ij}\} \tag{2.8}$$

and regarding it as a local Boltzmann weight, $\langle \Psi | \Psi \rangle$ can be interpreted as the partition function of a 2-layer 2D vertex model

$$Z^0 \equiv \sum_{[\eta]\,[\bar{\eta}]} \prod_{1 \le ij \le N} G^0\{\bar{\eta}_{ij} | \eta_{ij}\}\,. \tag{2.9}$$

(See Fig. 3.) In the same manner, $\langle \Psi | T | \Psi \rangle$ can be expressed as the partition function of a 3-layer 2D vertex model:

$$Z^1 \equiv \sum_{[\eta]\,[\sigma]\,[\bar{\eta}]} \prod_{1 \le ij \le N} G^1\{\bar{\eta}_{ij} | \sigma_{ij} | \eta_{ij}\}, \tag{2.10}$$

which is characterized by the local Boltzmann weight:

$$G^1\{\bar{\eta}_{ij} | \sigma_{ij} | \eta_{ij}\} \equiv \mathbf{V}\{\bar{\eta}_{ij}\} \cdot \left(W\{\sigma_{ij}\} \mathbf{V}\{\eta_{ij}\} \right) = \sum_{\bar{s}s} v^{\bar{s}}\{\bar{\eta}_{ij}\} w_{\bar{s}s}\{\sigma_{ij}\} v^s\{\eta_{ij}\}\,. \tag{2.11}$$

Thus once the $2m^4$ numbers of the elements (of $v^s\{\eta\}$) are given, the variational ratio $\lambda[\Psi] = Z^1/Z^0$ is easily obtained via standard numerical methods for the 2D classical lattice models. What we have to consider next is the way to find out the best tensor $v^s\{\eta\}$ which maximizes $\lambda[\Psi]$.

§3. Maximization of the Variational Partition Function

In order to maximize the variational partition function $\lambda[\Psi]$, we consider its variation:

$$\delta\lambda[\Psi] \equiv \sum_{ij} \frac{\partial \lambda[\Psi]}{\partial v^{\bar{s}}\{\bar{\eta}_{ij}\}} \delta v^{\bar{s}}\{\bar{\eta}_{ij}\} + \sum_{ij} \frac{\partial \lambda[\Psi]}{\partial v^s\{\eta_{ij}\}} \delta v^s\{\eta_{ij}\} \tag{3.1}$$

with respect to the infinitesimal change of the local tensors

$$v^{\bar{s}}\{\bar{\eta}_{ij}\} \rightarrow v^{\bar{s}}\{\bar{\eta}_{ij}\} + \delta v^{\bar{s}}\{\bar{\eta}_{ij}\}$$
$$v^s\{\eta_{ij}\} \rightarrow v^s\{\eta_{ij}\} + \delta v^s\{\eta_{ij}\}\,. \tag{3.2}$$

When the linear dimension of the system ($= N$) is sufficiently large, most of the terms in the r.h.s. of Eq. (3.1) are very close with each other. This is because the boundary is far away from most of the sites and hence the system can be regarded to be uniform in the thermodynamic limit. Thus it is sufficient to treat the variation of $\lambda[\Psi]$ at the center of the system:

$$\delta_{\rm c}\lambda[\Psi] \equiv \frac{\partial \lambda[\Psi]}{\partial v^{\bar{s}}\{\bar{\eta}_{\rm c}\}} \delta v^{\bar{s}}\{\bar{\eta}_{\rm c}\} + \frac{\partial \lambda[\Psi]}{\partial v^s\{\eta_{\rm c}\}} \delta v^s\{\eta_{\rm c}\}\,, \tag{3.3}$$

where $v^{\bar{s}}\{\bar{\eta}_{\rm c}\}$ and $v^s\{\eta_{\rm c}\}$ are tensors at the center c $= (N/2, N/2)$.

For the convenience of writing down $\delta_{\rm c}\lambda[\Psi]$ more explicitly, we divide $Z^0 = \langle \Psi | \Psi \rangle$ and $Z^1 = \langle \Psi | T | \Psi \rangle$ into two parts as follows:

$$Z^0 = \sum_{\{\bar{\eta}_{\rm c}\}\{\eta_{\rm c}\}} G^0\{\bar{\eta}_{\rm c} | \eta_{\rm c}\} X^0\{\bar{\eta}_{\rm c} | \eta_{\rm c}\}$$

$$Z^1 = \sum_{\{\bar{\eta}_{\rm c}\}\{\sigma_{\rm c}\}\{\eta_{\rm c}\}} G^1\{\bar{\eta}_{\rm c} | \sigma_{\rm c} | \eta_{\rm c}\} X^1\{\bar{\eta}_{\rm c} | \sigma_{\rm c} | \eta_{\rm c}\}\,. \tag{3.4}$$

The factors G^0 and G^1 are the "local Boltzmann weights" at the center of the system, and $X^0\{\bar{\eta}_c|\eta_c\}$ and $X^1\{\bar{\eta}_c|\sigma_c|\eta_c\}$ are the rest of the system. The new tensors $X^0\{\bar{\eta}_c|\eta_c\}$ and $X^1\{\bar{\eta}_c|\sigma_c|\eta_c\}$ play a role of "reservoirs" in the terminology of the DMRG, which are defined as

$$X^0\{\bar{\eta}_c|\eta_c\} \equiv \sum_{[\bar{\eta}]'\,[\eta]'} \prod_{(ij)\neq c} G^0\{\bar{\eta}_{ij}|\eta_{ij}\}$$

$$X^1\{\bar{\eta}_c|\sigma_c|\eta_c\} \equiv \sum_{[\bar{\eta}]'\,[\sigma]'\,[\eta]'} \prod_{(ij)\neq c} G^1\{\bar{\eta}_{ij}|\sigma_{ij}|\eta_{ij}\}\,, \qquad (3{\cdot}5)$$

where the restricted product $\prod_{(ij)\neq c}$ denotes that $G^0\{\bar{\eta}_c|\eta_c\}$ and $G^1\{\bar{\eta}_c|\sigma_c|\eta_c\}$ are not included in the right hand sides, and the restricted sum $\sum_{[\bar{\eta}]'\,[\eta]'}$ and $\sum_{[\bar{\eta}]'\,[\sigma]'\,[\eta]'}$ denote spin configuration sum for all the spins except for those at the center, $\bar{\eta}_c$, σ_c, and η_c. Thus the division by Eq. (3.4) is equivalent to punch out the system a the center; this operation is similar to puncture the system in the 'puncture renormalization group' by Martín-Delgado *et al.*[22]

Substituting the definitions of G^0 and G^1 into Eq. (3.4) and introducing two matrices

$$A_{\bar{s}s}\{\bar{\eta}_c|\eta_c\} \equiv \qquad X^0\{\bar{\eta}_c|\eta_c\}\,\delta_{\bar{s}s}$$

$$B_{\bar{s}s}\{\bar{\eta}_c|\eta_c\} \equiv \sum_{\{\sigma_c\}} X^1\{\bar{\eta}_c|\sigma_c|\eta_c\}\,w_{\bar{s}s}\{\sigma_c\} \qquad (3{\cdot}6)$$

we can express Z^0 and Z^1 in the binary form

$$Z^0 = \mathbf{V}_c^{\mathrm{T}} A\, \mathbf{V}_c \equiv \sum_{\bar{s}\,\{\bar{\eta}_c\}}\sum_{s\,\{\eta_c\}} v^{\bar{s}}\{\eta_c\} A_{\bar{s}s}\{\bar{\eta}_c|\eta_c\} v^s\{\eta_c\}$$

$$Z^1 = \mathbf{V}_c^{\mathrm{T}} B\, \mathbf{V}_c \equiv \sum_{\bar{s}\,\{\bar{\eta}_c\}}\sum_{s\,\{\eta_c\}} v^{\bar{s}}\{\eta_c\} B_{\bar{s}s}\{\bar{\eta}_c|\eta_c\} v^s\{\eta_c\} \qquad (3{\cdot}7)$$

of the $2m^4$-dimensional vector $\mathbf{V}_c$. Substituting the above expressions into Eq. (3.3), we finally obtain the stationary condition $\delta_c \lambda[\Psi] = 0$ expressed as a $2m^4$-dimensional generalized eigenvalue problem

$$\sum_{s\,\{\eta_c\}} B_{\bar{s}s}\{\bar{\eta}_c|\eta_c\} v^s\{\eta_c\} = \lambda[\Psi] \sum_{s\,\{\eta_c\}} A_{\bar{s}s}\{\bar{\eta}_c|\eta_c\} v^s\{\eta_c\}\,, \qquad (3{\cdot}8)$$

which can be abbreviated as $B\,\mathbf{V}_c = \lambda[\Psi]\,A\,\mathbf{V}_c$.

This is a non-linear equation for the tensors $v^{\bar{s}}\{\bar{\eta}\}$ and $v^s\{\eta\}$, because the 'matrices' A and B themselves are constructed from the tensors. Therefore, equation (3.8) should be interpreted as a self-consistent relation for the local tensors. A way to find out the solution of Eq. (3.8) is to repeat numerical substitutions as follows:

(a) Set a certain initial value to the tensor $\mathbf{V}$, which has $2m^4$ elements.
(b) Numerically calculate X^0 and X^1 by Eqs. (3.5). This calculation can be easily done with the help of the corner transfer matrix renormalization group (CTMRG).[18],[21],[23]

(c) Create A and B by Eqs. (3.6), and apply $A^{-1}B$ to the tensor to obtain $\mathbf{V}' = A^{-1}B\,\mathbf{V}$.

(d) Create a new variational tensor $\mathbf{V} + \epsilon\mathbf{V}'$ where ϵ is a small parameter. (We set $\epsilon = 0.1$.) Use $\mathbf{V} + \epsilon\mathbf{V}'$ as the new variational tensor and return to (b).

(e) Stop the calculation when $\lambda[\Psi]$ does not increase any more.

This numerical iteration works when the matrix A is regular and positive definite. This condition is at least satisfied in the neighborhood of the stationary point where $\lambda[\Psi]$ takes its maximum, but is not in general for arbitrary $\mathbf{V}$. Thus, the initial choice of the variational tensor $\mathbf{V}$ is relevant to the stability of the numerical calculation.

§4. Numerical Result

We perform a calculation for the simplest vertex-type TPS with $m = 2$. Note that each tensor has $2m^4 = 32$ elements, which is twice as many as that of the IRF-type TPS. [18] To start the numerical calculation, we set the initial tensor $v^s\{\eta\}$ from the vertex weight

$$v^s(\eta\,\eta'\eta''\eta''') = w_{+s}(\sigma\,\sigma'\sigma''\sigma''') + a\,w_{-s}(\sigma\,\sigma'\sigma''\sigma''') \qquad (4\cdot1)$$

where $a \sim 1$ is a constant that weakly breaks the spin inversion symmetry $s \to -s$ of the initial TPS; typically we set $a = 1.01$. The construction of the initial tensor explicitly uses the fact that $m = 2$. We then performed the numerical self-consistent improvement for $v^s\{\eta\}$, and have succeeded to reach the fixed point that satisfies Eq. (3.8) within 1000 iterations in the whole temperature regions.

In order to check the quality of the obtained TPS, we observe the spontaneous magnetization of the 3D Ising model. In the vertex representation of the 3D Ising model (Eq. (2.1)), the magnetization with respect to the optimized TPS is expressed as

$$M = \frac{\mathbf{V}_\mathrm{c}^\mathrm{T} O\,\mathbf{V}_\mathrm{c}}{\mathbf{V}_\mathrm{c}^\mathrm{T} A\,\mathbf{V}_\mathrm{c}}\left(\frac{\mathbf{V}_\mathrm{c}^\mathrm{T} B\,\mathbf{V}_\mathrm{c}}{\mathbf{V}_\mathrm{c}^\mathrm{T} A\,\mathbf{V}_\mathrm{c}}\right)^{-1} = \frac{\mathbf{V}_\mathrm{c}^\mathrm{T} O\,\mathbf{V}_\mathrm{c}}{\mathbf{V}_\mathrm{c}^\mathrm{T} B\,\mathbf{V}_\mathrm{c}}, \qquad (4\cdot2)$$

where the new matrix O is — similar to the matrix B — defined as

$$O_{\bar{s}s}\{\bar{\eta}_\mathrm{c}|\eta_\mathrm{c}\} \equiv \sum_{\{\sigma_\mathrm{c}\}} X^1\{\bar{\eta}_\mathrm{c}|\sigma_\mathrm{c}|\eta_\mathrm{c}\}\,o_{\bar{s}s}\{\sigma_\mathrm{c}\} \qquad (4\cdot3)$$

with the modified vertex weight

$$o_{\bar{s}s}\{\sigma\} = \sum_{x=\pm1} x\,U_{\bar{s}}^x\,U_s^x\,U_\sigma^x\,U_{\sigma'}^x\,U_{\sigma''}^x\,U_{\sigma'''}^x, \qquad (4\cdot4)$$

which represents polarization of the Ising spin at the center of the system.

We show the calculated result in figure 4. The black triangles indicates the calculated spontaneous magnetization $M^\mathrm{V}(K \equiv \beta J)$ by the vertex-type TPS. For comparison, we also show the magnetization $M^\mathrm{IRF}(K)$ calculated by the IRF-type variational formulation [18] (white squares) and the Monte Carlo result $M^\mathrm{MC}(K)$ (line) by Talapov and Blöte. [19] Away from the critical point, $M^\mathrm{V}(K)$ shows good
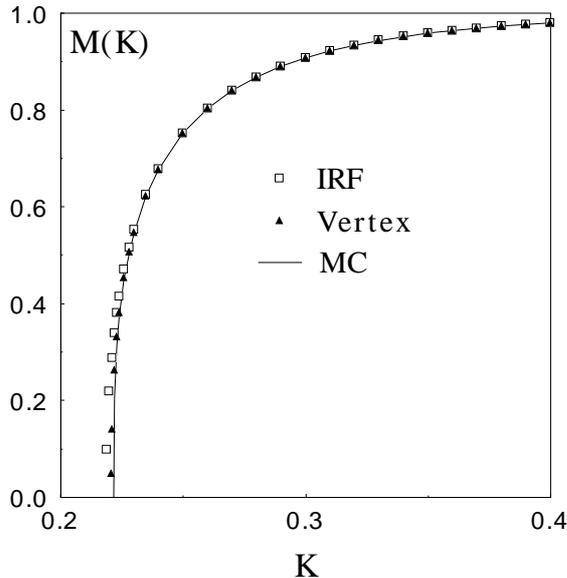
Fig. 4. Spontaneous magnetization $M^{\mathrm{V}}(K)$ of the 3D Ising model calculated via TPS when $m = 2$. (See black triangles.) For comparison, magnetization obtained by the IRF-type variational calculation [18] $M^{\mathrm{IRF}}(K)$ (white squares) and that by a Monte Carlo simulation [19] $M^{\mathrm{MC}}(K)$ (curve) are shown.

agreement with $M^{\mathrm{MC}}(K)$, but as K approaches to the critical point $M^{\mathrm{V}}(K)$ deviates from $M^{\mathrm{MC}}(K)$. The estimated critical point by the vertex-type TPS is $K_{\mathrm{c}}^{\mathrm{V}} = 0.2203$, which is 0.6% smaller than $K_{\mathrm{c}}^{\mathrm{MC}} = 0.2216544$ [19), 20]. We can see that the result for the vertex-type TPS is better than that for the IRF-type variational formulation $K_{\mathrm{c}}^{\mathrm{IRF}} = 0.2188$, which is 1.5% smaller than $K_{\mathrm{c}}^{\mathrm{MC}}$. Thus we can conclude that vertex-type TPS is more efficient than the IRF-type TPS. [18] We note that the observed critical behavior of $M^{\mathrm{V}}(K)$ in the vicinity of the critical point is the mean-field one $M^{\mathrm{V}}(K) \propto \sqrt{K - K_{\mathrm{c}}^V}$. It should be remarked that the numerical computation time with the vertex formulation is the same order as that of the IRF one.

§5. Conclusions and Discussions

We have proposed a numerical self-consistent method for 3D classical systems, which optimizes the 2D vertex-type TPS with $2m^4$ variational parameters. The method is applied to the 3D vertex model, which has the same thermodynamic property with the 3D Ising model, and we have confirmed that the vertex-type TPS gives better transition temperature than the IRF-type TPS.

If we increase the number of states m of the auxiliary variables of the vertex-type TPS we will be able to further tune the vertex-type TPS. It is possible to make a calculations of A and B in Eq. (3.6) with a short computation of a few seconds up to $m \sim 4$. We have, however, not succeeded in finding out the solution of the self-consistent equation (Eq. (3.8)) stably for the cases $m > 2$. This is because we

encounter a numerical problem that the matrix A becomes singular during the self-consistent calculation. It is our future problem to find out a systematic way to set up the initial tensor so that A is always regular and positive definite.

Acknowledgments

References

1) H.A. Kramers and G.H. Wannier, Phys. Rev. **60** (1941), 263.
2) L. Onsager, Phys. Rev. **65** (1944), 117.
3) R.J. Baxter, J. Math. Phys. **9** (1968), 650.
4) R.J. Baxter, J. Stat. Phys. **19** (1978), 461.
5) R.J. Baxter, *Exactly Solved Models in Statistical Mechanics* (Academic Press, London, 1982), p.363.
6) S.R. White, Phys. Rev. Lett. **69** (1992), 2863.
7) S.R. White, Phys. Rev. **B48** (1993), 10345.
8) *Density-Matrix Renormalization — A New Numerical Method in Physics,* Lecture notes in Physics, eds. I. Peschel, X. Wang, M. Kaulke, and K. Hallberg (Springer Verlag, 1999).
9) M. Fannes, B. Nachtergale and R.F. Werner, Europhys. Lett. **10** (1989), 633.
10) M. Fannes, B. Nachtergale and R.F. Werner, Commun. Math. Phys. **174** (1995), 477.
11) S. Östlund and S. Rommer, Phys. Rev. Lett **75** (1995), 3537; S. Rommer and S. Östlund, Phys. Rev. **B55** (1997), 2164.
12) G. Sierra and M.A. Martín-Delgado, cond-mat/9811170.
13) T. Nishino and K. Okunishi, J. Phys. Soc. Jpn. **68** (1999), 3066.
14) H. Niggemann, A. Klümper and J. Zittartz, Z. Phys. **B104** (1997), 103.
15) H. Niggemann, A. Klümper and J. Zittartz, Eur. Phys. J. **B13** (2000), 15.
16) Y. Hieida, K. Okunishi and Y. Akutsu, New J. Phys. **1** (1999), 7.
17) K. Okunishi and T. Nishino, Prog. Theor. Phys.**103** (2000), 541.
18) T. Nishino, K. Okunishi, Y. Hieida, N. Maeshima and Y. Akutsu, Nucl. Phys. **B575** (2000), 504.
19) A.L. Talapov and H.W.J. Blöte, J. Phys. A, Math. Gen. **29** (1996), 5727.
20) A.M. Ferrenberg and D.P. Landau, Phys. Rev. **B44** (1991), 5081.
21) T. Nishino and K. Okunishi, J. Phys. Soc. Jpn. **66** (1997), 3040.
22) M.A. Martín-Delgado, J. Rodriguez-Laguna, and G. Sierra, cond-mat/0009474.
23) T. Nishino and K. Okunishi, J. Phys. Soc. Jpn. **65** (1996), 891.